ISSN 1063-7761, Journal of Experimental and Theoretical Physics, 2008, Vol. 106, No. 4, pp. 800–805. © Pleiades Publishing, Inc., 2008.
Original Russian Text © Y.V. Kislinskii, K.Y. Konstantinian, G.A. Ovsyannikov, P.V. Komissinskiy, I.V. Borisenko, A.V. Shadrin, 2008, published in Zhurnal Éksperimental'noĭ i Teoreticheskoĭ Fiziki, 2008, Vol. 133, No. 4, pp. 914–920.

ELECTRONIC PROPERTIES OF SOLIDS

Magnetically Dependent Superconducting Transport in Oxide Heterostructures with an Antiferromagnetic Layer

Y. V. Kislinskii[a], K. Y. Konstantinian[a,*], G. A. Ovsyannikov[a,b], P. V. Komissinskiy[a,b,c], I. V. Borisenko[a], and A. V. Shadrin[a]

[a] *Institute of Radio Engineering and Electronics, Russian Academy of Sciences, Moscow, 125009 Russia*
**e-mail: karen@hitech.cplire.ru*
[b] *Chalmers University of Technology, Gothenburg, SE-41296 Sweden*
[c] *Darmstadt University of Technology, Darmstadt, D-64287 Germany*

Received August 30, 2007

Abstract—The superconducting current in hybrid superconducting structures $Nb/Au/Ca_{1-x}Sr_xCuO_2/YBa_2Cu_3O_{7-\delta}$ with an antiferromagnetic layer is experimentally shown to have a Josephson nature, and the deviation from the sinusoidal dependence of the superconducting current on the phase difference between superconducting electrodes is about 20% of the second harmonic. These heterostructures are found to have sensitivity to an applied magnetic field that is much higher than that of conventional Josephson junctions. The experimental shape of the magnetic-field dependence of the critical current in the heterostructures differs from the usual Fraunhofer shape by oscillation with a significantly smaller period along a magnetic field.

PACS numbers: 74.45.+c, 74.50.+r, 75.70.Cn

DOI: 10.1134/S1063776108040201

1. INTRODUCTION

Multilayer hybrid superconducting structures with an interlayer consisting of alternating ferromagnet (F), normal metal (N), and insulator (I) layers have aroused considerable interest [1–4]. The current in such structures can be controlled due to the rotation of the magnetization direction in the F layers in a weak magnetic field. Similar processes can occur in an antiferromagnetic (AF) layer, which can be considered as a set of ferromagnetic atomic-thick layers with oppositely directed magnetizations [5, 6]. As was theoretically shown in [5], an S–AF–S structure (S denotes a superconductor) with a layer of an A-type antiferromagnet has a critical current I_c. This current depends on the applied magnetic field H, which changes the AF-interlayer parameters,

$$I_c(H) \approx I_c^0\left(\frac{2}{\pi\beta M_S}\right)^{1/2}\left|\cos\left(\beta M_S - \frac{\pi}{4}\right)\right|, \qquad (1)$$

where $\beta \gg 1$ characterizes the electronic structure of the AF layer; $0 < M_S < 1$ is the antiferromagnetic order parameter, which depends on the spatial components of the local magnetization of the F layers and the applied magnetic field H; and I_c^0 is the critical current in the absence of a magnetic field, which coincides with the value of I_c in an equivalent S–N–S structure [5]. The authors of [5] also showed that the damping of the superconducting order parameter in the AF layer is specified by its metallic conduction; in the clean limit, the coherence length is $\xi_{AF} = hv_F/kT$, where v_F is the Fermi velocity in the layer; T is the temperature; and h and k are the Planck and Boltzmann constants, respectively.

As follows from Eq. (1), the period of the $I_c(H)$ dependence for an S–AF–S structure differs substantially from the period of the Fraunhofer dependence typical of a Josephson junction with a homogeneous barrier layer [7],

$$I_c(H) = I_c^0\left|\frac{\sin(\pi\Phi/\Phi_0)}{\pi\Phi/\Phi_0}\right|, \qquad (2)$$

where $\Phi = \mu_0 HA$ is the magnetic flux penetrating into the Josephson junction, μ_0 is the magnetic constant, $A = Ld_e$ is the cross-sectional area of the Josephson junction, $d_e = \lambda_{L1} + \lambda_{L2} + t$ is the effective magnetic-field penetration depth in the Josephson junction, λ_{Li} are the London penetration depths of the magnetic field in the electrodes forming this junction ($i = 1, 2$), t is the interelectrode barrier thickness, and L is the geometric size of the Josephson junction. The zeros of the $I_c(H)$ dependence in Eq. (2) correspond to an integer number of magnetic-flux quanta entering into the Josephson junction, $\Phi_0 = h/2e = 2.07 \times 10^{-15}$ Wb, where e is the electron charge. At the same time, Eq. (1) demonstrates that the zeros of $I_c(H)$ correspond to the condition $\beta M_S =$

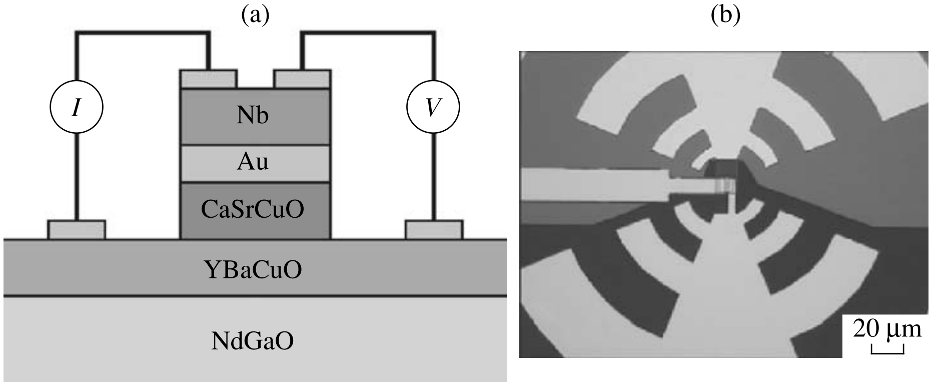

Fig. 1. (a) Cross section of a structure with an AF layer. The layer thicknesses are as follows: YBaCuO, 200 nm; CaCrCuO, 20–50 nm; Au, 10–20 nm; Nb, 200 nm. (b) Top view of the structure; the bright background indicates the superconducting electrodes of a log-periodic antenna and a lateral tap used for four-probe resistance measurements.

$\pi/4 + \pi n$ (n = 1, 2, …). Then, in the case $\beta \gg 1$ $I_c(H)$ oscillations can be detected at low fields (see Eq. (1)) [5].

Fraunhofer-type $I_c(H)$ dependences were observed in most lumped Josephson junctions, which satisfy the condition $L < 4\lambda_J$, where λ_J is the Josephson penetration depth of the magnetic field, which depends on the superconducting-current density j_c,

$$\lambda_J = \left(\frac{h}{4\pi e\mu_0 d_e j_c}\right)^{1/2}. \qquad (3)$$

For distributed Josephson junctions ($L > 4\lambda_J$), $I_c(H)$ usually deviates from the Fraunhofer shape [7].

The first experimental data on a Josephson current in an S–AF–S structure were obtained on Nb-based junctions with an FeMn layer [8]. As H increased, the $I_c(H)$ dependence was nonmonotonic and close to Fraunhofer-type Eq. (2). The London penetration depth in superconducting electrodes determined from the zeros of $I_c(H)$ (λ_L = 40 nm) was found to be close to the tabulated value for Nb (λ_L = 47 nm). The secondary $I_c(H)$ maximum amplitudes were nearly twice as large as the expected Fraunhofer amplitudes, which could be caused by both a change in the magnetization of the AF layer (as follows from Eq. (1)) and by a nonuniform distribution of the superconducting-current density and the local magnetization of the layers because of the polycrystalline structure of the AF layer. Coherence length ξ_{AF} was experimentally shown to be specified by the Néel temperature (100–300 K) rather than the physical temperature (about 4 K).

In this work, we experimentally study the magnetic-field characteristics of hybrid heterostructures $Nb/Au/Ca_{1-x}Sr_xCuO_2/YBa_2Cu_3O_{7-\delta}$ based on epitaxial films of the oxide superconductor $YBa_2Cu_3O_{7-\delta}$ (YBCO) with the d-wave symmetry of the order parameter (D superconductor). Niobium (Nb) is a conventional metallic superconductor; Au is a gold film used to decrease the oxygen diffusion from YBCO; and the $Ca_{1-x}Sr_xCuO_2$ (CSCO) layer is a quasi-two-dimensional Heisenberg antiferromagnet at low temperatures with a Néel temperature of 100 K [9, 10]. In [11, 12], we studied the anomalous proximity effect and the Josephson nature of the critical current in such D–AF–S oxide heterostructures and presented preliminary data on their microwave and magnetic-field dependences.

Note that the d-wave symmetry of the order parameter in YBCO can change the $I_c(H)$ dependence [13] and that the interpretation of the $I_c(H)$ measurement results is substantially complicated by the anisotropy of the London penetration depth and by a change in the level of doping at the interface near the superconductor layers, which specify λ_{Li} [14–16]. In this case, however, the authors of [14] observed good experimental agreement between $I_c(H)$ and Fraunhofer Eq. (2) with allowance for the inhomogeneity of the tunneling layer in the hybrid junctions based on $YBa_2Cu_3O_{7-\delta}$ films.

2. EXPERIMENTAL

The CSCO/YBCO epitaxial heterostructures were evaporated onto $NdGaO_3$ substrates by laser ablation at a temperature T = 800°C. After cooling, an Au film was deposited without a break in the vacuum. We used CSCO compositions with x = 0.15 and 0.50. The AF layer thickness varied in the range d_S = 20–50 nm. The Nb and additional Au layers were deposited by magnetron sputtering. The topology of the structure was formed by photolithography, plasmachemical etching, and ion-beam etching [11–13]. Figure 1a shows the cross section of the structure, and its shape represented a square with linear sizes L = 10–50 μm involved in a log-periodic antenna used to measure millimeter-range wavelengths in an electromagnetic field (Fig. 1b). To measure the electrophysical characteristics of the structure, we applied two contacts onto the top Nb electrode and two contacts onto the YBCO film (Fig. 1a). In this case, at $T < T_c$ (T_c is the critical temperature of the YBCO film), we measured the resistances of the CSCO layer and the Au/CSCO interface by the four-probe

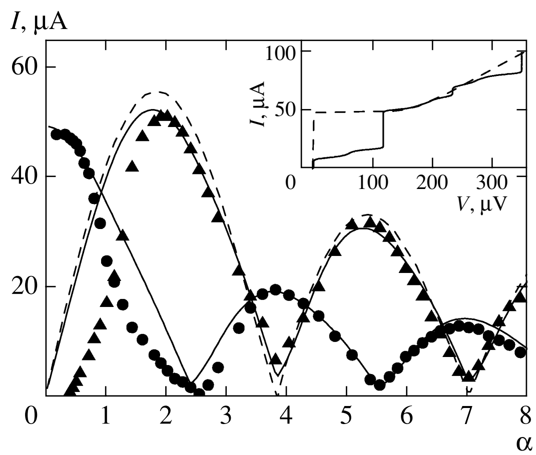

Fig. 2. Dependences of (circles) critical current $I_c(\alpha)$ and (triangles) first Shapiro step $I_1(\alpha)$ on the normalized amplitude $\alpha \approx I_{RF}/I_c(0)$ of millimeter-range radiation with a frequency of 56 GHz. The dashed lines illustrate the theoretical $I_1(\alpha)$ dependence obtained from the resistive model of a Josephson junction. The solid line illustrates the dependences calculated with allowance for the second harmonic of the current–phase relation at $q = 0.2$. The inset shows the I–V characteristic of an Nb/Au/CSCO/YBCO heterostructure: (dashed line) intrinsic characteristic and (solid line) under the action of electromagnetic radiation.

method. According to our preliminary measurements performed in [11, 12], the resistances of the Au, Nb, and CSCO films and the CSCO/YBCO interface may be neglected. As a result, the fabricated structures with an AF layer can be considered as S–N–I_b–AF–D junctions, where the Au/CSCO interface plays the role of the I_b barrier. For comparison, we used the same technique to prepare and study Nb/Au/YBCO hybrid heterostructures without an AF layer. The structures of both types were measured under the same conditions. To investigate magnetic-field dependences in low fields, we used an additional shield made of an amorphous permalloy.

3. RESULTS AND DISCUSSION

At low voltages ($V \leq 1$ mV), the shape of the I–V characteristics of the heterostructures is close the hyperbolic shape typical of Josephson junctions (Fig. 2, inset). At voltages $V \geq 5$ mV and temperatures $T_c > T > T_c'$ (T_c' is the critical temperature of the niobium film), the conductivity exhibits an anomaly with a maximum at $V = 0$, which is most likely to be caused by low-energy Andreev bound states [11, 12]. At $T < T_c'$, the voltage dependences of the differential resistance of the heterostructures ($R_d(V)$) have specific features induced by the superconducting gap in niobium. On the whole, the temperature dependence of the critical current of the entire structure ($I_c(T)$) follows the temperature dependence of superconducting parameter Δ_{Nb} in the Nb film as in structures without an AF layer [13]. The absence of a quadratic increase in the critical current with decreasing temperature and the weak dependence of the characteristic voltage of the structure $V_c = I_cR_N$ (I_c is the critical current, and R_N is the normal resistance of the structure) on the CSCO layer thickness (see table) indicate that the layer thickness is small and that the condition $\xi_{AF} \ll d_S$, which determines the exponential dependence of the critical current, is not met [17]. Since thickness d_S in all structures with an AF layer under study is several tens of nanometers, the penetration depth of a superconducting order parameter in CSCO is significantly larger than that detected for an FeMn polycrystalline layer in [8].

When the heterostructures are subjected to monochromatic radiation with a millimeter-range wavelength, Shapiro steps, which are caused by the synchronization of their radiation by an external signal, appear

Table

No.	d_S, nm	x	L, μm	I_c, μA	R_N, Ω	V_c, μV	$\mu_0\Delta H$, μT	λ_J, μm
274-10	50	0.5	10	2.5	60	150	54	196
274-20	50	0.5	20	10	20	200	9	196
274-30	50	0.5	30	18	9.8	176	5	219
274-40	50	0.5	40	51	4.2	214	6	174
274-50	50	0.5	50	70	2.9	203	3	185
269-20	50	0.15	20	280	0.38	106	12	37
273-10	20	0.5	10	335	0.8	268	38	18
273-20	20	0.5	20	890	0.15	134	49	21
N2-20	0	–	20	20	3.6	72	139	162
N2-30	0	–	30	60	0.93	56	118	140
N2-50	0	–	50	198	0.44	87	56	129

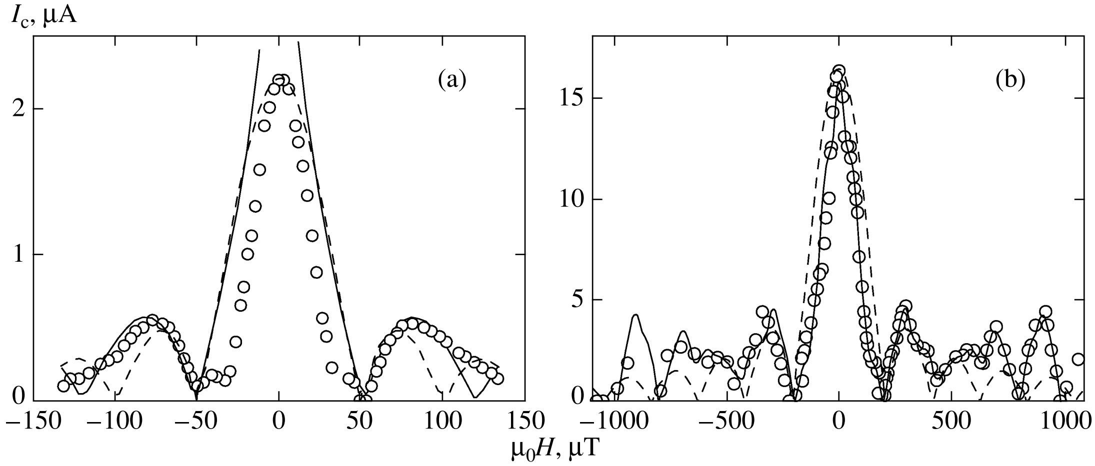

Fig. 3. (a) Magnetic-field dependence of the critical current $I_c(H)$ of a heterostructure of size L = 10 μm with an AF layer: (solid line) calculation using Eq. (1) and (dashed line) Fraunhofer Eq. (2). (b) $I_c(H)$ for a structure of size L = 20 μm without an AF layer (Nb/Au/YBCO): (dashed line) Fraunhofer Eq. (2) and (solid line) numerical calculation [14].

in their I–V characteristics (Fig. 2, inset). The oscillation dependences of the critical current and the first Shapiro step on the normalized external-signal amplitude $\alpha = I_{RF}/I_c$ support the Josephson nature of the superconducting current (Fig. 2). The critical frequency $f_c = 2eV_c/h$ = 50 GHz, which was determined from the maximum value of the first Shapiro step using a resistive model (Fig. 2, dashed line), agrees satisfactorily with f_c = 70 GHz, which was calculated from the value obtained upon dc measurement (I_cR_N = 145 μV), indicating a uniform current in the structure and the absence of pinholes. The best agreement between the maximum value of the first Shapiro step and the calculated value is achieved when the second harmonic (sin2φ) in the $I_S(\varphi) = I_{c1}\sin\varphi + I_{c2}\sin 2\varphi$ dependence of the superconducting current is taken into account. According to the calculation in terms of the modified resistive model in [13] (which takes into account the presence of I_{c2}; Fig. 2, solid line), the amplitude ratio of the second to first harmonic for the structure shown in Fig. 2 is $q = I_{c2}/I_{c1} = 0.2$.

Figure 3a shows the $I_c(H)$ dependence for a structure of size L = 10 μm with an AF layer made of a CSCO film of thickness d_S = 50 nm and x = 0.5. The dashed line in Fig. 3a illustrates the dependence plotted according to Eq. (2) from the experimental data normalized by critical current I_c^0 (T = 4.2 K) and the first zero of the magnetic field dependence (H_1). The position of the second zero of the experimental dependence (H_2) is seen to differ significantly from Fraunhofer Eq. (2). The solid line in Fig. 3a illustrates Eq. (1) at experimental parameters I_c^0 and H_1 and an exponent of –0.75 rather than –0.5 (as in the theory of [5]) for the coefficient $(2/\pi\beta M_S)$ in Eq. (1). The deviation of experimental points from the solid line in Fig. 3a at low H is caused by the limitation of the applicability of Eq. (1) at M_S close to zero [5]. For comparison, Fig. 3b shows the $I_c(H)$ dependence for the heterostructure without the AF layer. In this case, the deviation of the experimental $I_c(H)$ dependence from the Fraunhofer dependence is seen to occur at higher values of the applied magnetic field ($H > H_2$). The value of d_e estimated from the measured value of H_1 ($d_e = \Phi_0/\mu_0 H_1 L$ = 0.5 μm) yields λ_{L1} = 0.38 μm, which is higher than the tabular value for optimally doped YBCO (λ_{L1} = 0.15 μm) [18]. This difference is likely to be caused by the demagnetizing factor of the structure geometry. Note that the data given in Fig. 3 were obtained when a magnetic field was applied normal to the heterostructure plane [19]. We detected no substantial changes in the shape of the $I_c(H)$ dependences measured experimentally in two different magnetic-field directions, namely, perpendicular to the heterostructure plane and along the YBCO electrode, and the demagnetizing factor only led to a change in the scale along H for these directions.

A comparison of the data in Figs. 3a and 3b demonstrates that, although the size L of the structure with an AF layer is half that of the structure without an AF layer, H_1 is significantly lower than the first-minimum field for the latter structure. In structures with x = 0.5 for L > 20 μm, this difference increases and reaches about 20 times, as determined for several samples (see table). This decrease by more than an order of magnitude in the magnetic field (H_1) required for the first minimum in the $I_c(H)$ dependence in the structures with a CSCO layer as compared to the structures without this layer can be related to the AF layer, since the measurements were carried out under the same experimental conditions on samples with the same geometry. Note that, for structures with x = 0.15, H_1 (and, hence, average I_c oscillation period ΔH) also decreases but to a lesser extent as compared to x = 0.5 (see table).

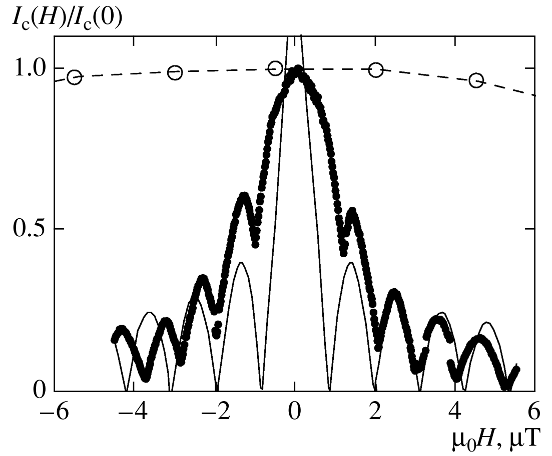

Fig. 4. (solid circles) Magnetic-field dependence of $I_c(H)$ for a structure of size $L = 50$ µm with an AF layer and (solid line) calculation using Eq. (1). (open circles) Fragment of the $I_c(H)$ dependence for the structure without an AF layer of the same size (given for comparison).

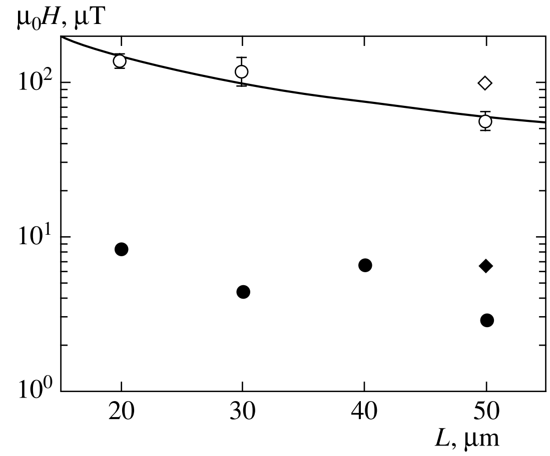

Fig. 5. Average peak width $\mu_0\Delta H$ vs. the heterostructure size: (open symbols) without (solid symbols) with an AF layer. (circles) The field is normal to the substrate (the measurement error is represented by the root-mean-square deviation); (diamonds) the field is parallel to the substrate plane along the antenna axis. (solid line) $\Delta H \propto 1/L$ approximation.

This significant decrease in H_1 cannot be explained by an increase in the London penetration depth λ_{L1} in YBCO because of a decrease in the level of oxygen doping of the YBCO film next to the Au/CSCO barrier layer (no more than 30% for the critical temperature of YBCO, which is 40 K) [11]. As follows from the broadened secondary maxima, the periodicity of the $I_c(H)$ shape for the structures with an AF layer (Fig. 3a) is closer to Eq. (1) with $H_1 \approx (H_2 - H_1)/2$, whereas, for the Fraunhofer dependence following from Eq. (2), $H_1 \approx (H_2 - H_1)$. Note that the $I_c(H)$ dependence for the structure without an AF layer is well described by the model in [13], which takes into account the presence of S/D nanocontacts to the (001) and (110) plane of the D superconductor in the barrier layer (Fig. 3b, solid line). According to [5], a nonmonotonic $I_c(H)$ dependence with a periodicity other than the magnetic-flux quantum in S–AF–S junctions is caused by a weak change in the canting of the magnetic moments in the ferromagnetic layers (and, correspondingly, in parameter M_S in Eq. (1)) in an applied magnetic field. $I_c(H)$ minima are detected at applied magnetic fields that are substantially lower than the field $H_1 = \Phi_0/\mu_0 d_e L$, which corresponds to the penetration of a magnetic-flux quantum Φ_0 into the structure.

As the size increases ($L > 20$ µm), the $I_c(H)$ dependences change: the critical current exhibits a maximum at low H, and $I_c(H)$ then decreases in an oscillation manner at a period of about 1 µT (see Fig. 4). At $L = 50$ µm, the shape of the $I_c(H)$ dependence seems to correspond to the case of a distributed Josephson junction, although the distribution condition $L > 4\lambda_J$ is not met. The periodicity of this oscillating "fine structure" of $I_c(H)$ is well described by Eq. (1), which is illustrated with a solid line in Fig. 4.

For the structures without an AF layer, the averaged field period ΔH of $I_c(H)$ oscillations decreases in proportion to $1/L$ (Fig. 5), and, for the structures with an AF layer, we failed to determine the exact L dependence of ΔH because of the complex shape of the $I_c(H)$ dependence at $L > 20$ µm. Note that, in all structures with an AF layer, ΔH decreases significantly with small deviations depending on the level of layer doping x (see table).

The high sensitivity of the heterostructures with an AF layer to an applied magnetic field can be used to solve applied problems. For example, the conversion of a magnetic field into voltage $\partial V/\partial(\mu_0 H)$ in a structure is an important characteristic for a SQUID-based magnetic transducer. We use the family of I–V characteristics induced by a magnetic field and the $I_c(H)$ dependence for a structure with $L = 10$ µm and obtain $\partial V/\partial(\mu_0 H) = 2.5$ V/T at $T = 4.2$ K. This value is close to the value $\partial V/\partial(\mu_0 H) = 2$ V/T) detected at the same temperature for SQUIDs on a bicrystal with a loop area of 200 µm^2 without an additional magnetic-flux concentrator [20].

4. CONCLUSIONS

We measured the superconducting current in hybrid oxide superconducting structures with an antiferromagnetic layer and showed that it has a Josephson nature. We revealed a deviation of the superconducting current–phase relation from a sinusoidal shape due to the presence of a 20% contribution of the second harmonic (~sin2φ). In contrast to the well-known Josephson structures, we observed critical-current modulation, which is induced by the effect of an applied magnetic field on the magnetization of the antiferromagnetic layer. As a result, the sensitivity of the structures to an applied magnetic field increases by almost an order of magnitude.

ACKNOWLEDGMENTS

We thank D. Winkler, V.V. Demidov, A.V. Zaitsev, and I.I. Solov'ev for fruitful discussions.

This work was supported by the Department of Physical Sciences of the Russian Academy of Sciences, the Ministry of Education and Science of the Russian Federation, European Union (project no. NMP3-CT-2006-033191), the European Scientific Foundation (projects AQDJJ, THIOX), the International Science and Technology Center (project no. 3743), and the Swedish KVA program.

REFERENCES

1. F. S. Bergeret, A. F. Volkov, and K. B. Efetov, Rev. Mod. Phys. **77**, 1321 (2005).
2. A. V. Zaitsev, Pis'ma Zh. Éksp. Teor. Fiz. **83** (6), 277 (2006) [JETP Lett. **83** (6), 233 (2006)].
3. T. Yu. Karminskaya and M. Yu. Kupriyanov, Pis'ma Zh. Éksp. Teor. Fiz. **86** (1), 65 (2007) [JETP Lett. **86** (1), 61 (2007)].
4. B. Crouzy, S. Tollis, and D. A. Ivanov, cond-mat/0706.1638.
5. L. P. Gorkov and V. Z Kresin, Phys. Rep. **400**, 149 (2004).
6. B. M. Andersen, I. V. Bobkova, P. J. Hirschfeld, and Yu. S. Barash, Phys. Rev. Lett. **96**, 117005 (2006).
7. A. Barone and G. Paterno, *Physics and Applications of the Josephson Effect* (Wiley, New York, 1982; Mir, Moscow, 1984).
8. C. Bell, E. J. Tarte, G. Burnell, et al., Phys. Rev. B: Condens. Matter **68**, 144517 (2003).
9. G. A. Ovsyannikov, S. A. Denisyuk, and I. K. Bdikin, Fiz. Tverd. Tela (St. Petersburg) **47** (3), 417 (2005) [Phys. Solid State **47** (3), 429 (2005)].
10. G. A. Ovsyannikov, V. V. Demidov, Y. V. Kislinskii, and P. V. Komissinskiy, in *Proceedings of the X Symposium on Nanophysics and Nanoelectronics, Nizhni Novgorod, Russia, 2006*, Vol. 2, p. 277 [in Russian].
11. G. A. Ovsyannikov, I. V. Borisenko, P. V. Komissinskiy, et al., Pis'ma Zh. Éksp. Teor. Fiz. **84** (5), 320 (2006) [JETP Lett. **84** (5), 262 (2006)].
12. P. Komissinskiy, G. A. Ovsyannikov, I. V. Borisenko, et al., Phys. Rev. Lett. **99**, 017004 (2007).
13. A. G. Sun, A. Truscott, A. S. Katz et al., Phys. Rev. B: Condens. Matter **54**, 6734 (1996).
14. Yu. V. Kislinskii, P. V. Komissinskiy, K. Y. Constantinian, et al., Zh. Éksp. Teor. Fiz. **128** (3), 575 (2005) [JETP **101** (3), 494 (2005)].
15. H. Akoh, C. Camerlingo, and S. Takada, Appl. Phys. Lett. **56**, 1487 (1990).
16. J. Yoshida, T. Hashimoto, S. Inoue, et al., Jpn. J. Appl. Phys. **31**, 1771 (1992).
17. K. A. Delin and A. W. Kleinsasser, Supercond. Sci. Technol. **9**, 227 (1996).
18. M. R. Trunin, Usp. Fiz. Nauk **175** (10), 1017 (2005) [Phys. Usp. **48** (10), 979 (2005)].
19. I. Rosenstein and J. T. Chen, Phys. Rev. Lett. **35**, 303 (1975).
20. Z. G. Ivanov, P. A. Nilsson, D. Winkler et al., Appl. Phys. Lett. **59**, 3030 (1991).

Translated by K. Shakhlevich